SHARAD MULTIBAND ANALYSIS OF RADAR SURFACE REFLECTIVITY IN THE MARTIAN POLAR LAYERED DEPOSITS. Erica R. Jawin[1], Bruce A. Campbell[1], [1]Smithsonian National Air and Space Museum, Washington, DC, USA (jawine@si.edu).

Introduction: The martian north and south polar layered deposits (PLD) are composed of ice and dust layers up to several kilometers thick and cover areas ~10^6 km^2 [*1*, *2*]. Although both PLDs are similarly dominated by water ice, radar reflectivity maps from the Shallow Radar (SHARAD) [*3*] reveal differences in peak echo power, where Planum Australe (SPLD) is about two-fold, or 3 dB, brighter than Planum Boreum (NPLD) [*4*]. [*4*] argue that the difference could be due to variations in surface roughness and the near-surface structures of the north and south PLDs: Planum Boreum contains ~300 m of bright, densely layered radar reflectors, while Planum Australe contains few reflectors which, when present, are weaker and have larger separations.

To investigate the difference in PLD surface reflectivity and near-surface structure, we used full bandwidth SHARAD data and processed multiband data to search for evidence of radar interference that could affect the surface echo power. [*5*] used SHARAD multiband data to investigate interference in Gemina Lingula in the NPLD, and found that the same reflector can vary in peak power by ~5 dB due to interference.

These observations are critical in disentangling the geologic evolution of the martian poles, and variations in their most recent evolution can provide insight into the global climate in the recent past. Additionally, if we can determine which of the PLDs better represents a single reflection off a near-planar target composed of pure water ice, that location would represent the best target to use as a radar calibration site with a known dielectric constant of ~3.15.

Data: SHARAD full-bandwidth data have a 10 MHz bandwidth spanning 15 to 25 MHz, with a free-space vertical resolution of 15 m [*6*]. The range resolution is modulated by the medium dielectric constant as $1/\sqrt{\epsilon}$, so the nominal range resolution in water ice ($\epsilon = 3.12$) is 8.5 m, in CO_2 ice ($\epsilon = 2.1$) is 10.4 m, and in solid rock ($\epsilon = 8$) is 5.3 m.

SHARAD multiband data split the 10 MHz bandwidth into sub-bands centered at 17.5 MHz ("low frequency" or L band) and 22.5 MHz ("high frequency" or H band), with a range resolution of ~20 m in ice [*7*]. Separate radargrams are produced for each sub-band which show different scattering behavior due to their different frequencies. Sub-band variations in echo strength are expressed in terms of the ratio of power in the two bands, P_{High}/P_{Low} ("H" and "L" are in terms of wavelength). Smooth, planar surfaces should result in H/L near unity, or 0 dB, such as the smooth equatorial regions of Mars [*7*]. Closely-spaced reflectors can lead to interference (either constructive or destructive, when reflector spacing approaches one-half or one-quarter wavelength, respectively), generating H/L values that differ from unity, such as in Gemina Lingula in the NPLD [*5*].

Results: We calculated maps of H/L for several hundred SHARAD tracks over both poles. Both PLDs show regions where H/L is approximately equal (yellow regions and light green/light purple in **Figure 1**). The SPLD is dominated by such regions, specifically in

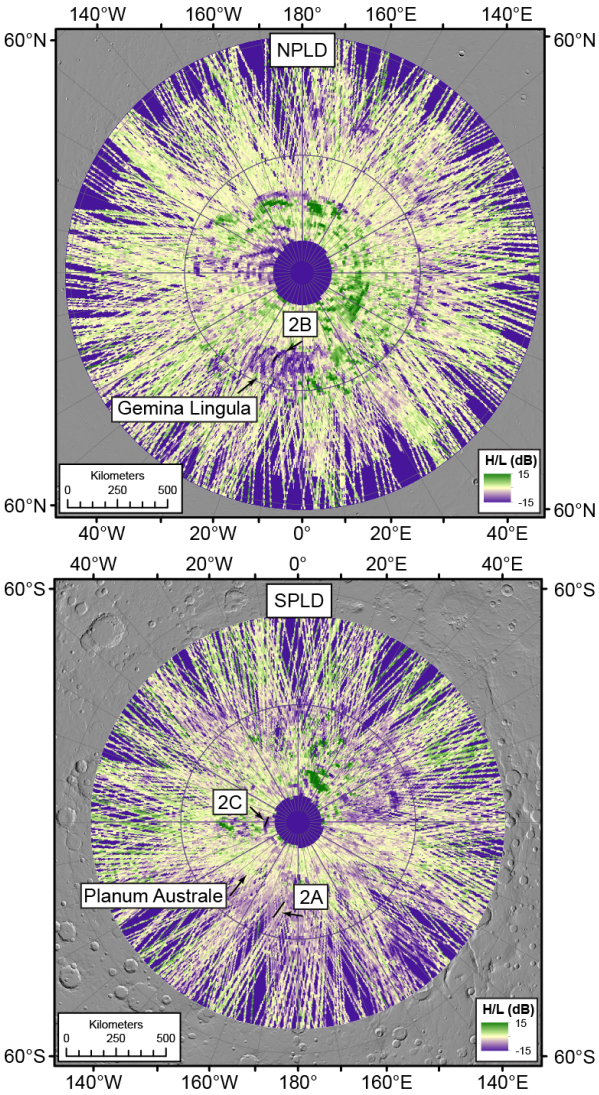

Figure 1. Relative surface echo power in H and L bands over the polar regions. Values that deviate strongly from 0 dB indicate potential interference. Large purple regions such as those at the poles indicate data gaps.

Planum Australe which has a strong surface reflection, few near-surface reflectors, and near-equal power in both H and L bands (**Figure 2A**). In contrast, the NPLD contains many regions where the surface echo H/L ratio is ± several dB (dark green and purple regions, **Figure 1**), indicating a stronger return in either the H or L sub-band (**Figure 2B**).

Several isolated regions of the SPLD show apparent non-unity H/L values (**Figure 1**). However, unlike the NPLD, some of these regions have strong subsurface reflections that exceed the power of the surface reflection in full-BW data, so the inference of multi-band surface returns may be incorrect (**Figure 2C**). The distribution of these non-unity H/L regions is similar to that of reflection-free zones (RFZs) which are believed to contain CO_2 ice [*8*, *9*].

Discussion: The difference in H/L behavior between the north and south PLDs (**Figure 2A-B**) appears to be correlated to the presence (and absence, respectively) of bright, closely-spaced, near-surface reflectors. The presence of non-unity H/L in the NPLD suggests that interference partly explains the reflectance variations at both PLDs, although as noted by [*4*], surface roughness at the wavelength scale (among other properties) can also affect the reflectivity.

By comparing the first echo from the surface of the north and south PLD, we can effectively compare the top ~20 m (in the multiband data) of both polar settings. The NPLD's dense near-surface layering (**Figure 2B**) argues for a variable climate which experienced periods of accumulation and ablation, resulting in the formation of layer(s) of dust-rich and dust-poor ice within the uppermost ~20 m of the surface. The NPLD has likely been modified in the very recent past, with a crater retention age of ~1,500 years [*10*]. The deposition of the uppermost ~20 m of Planum Australe must have been less variable, lacking periods of enhanced dust deposition and/or periods of sufficient ice ablation necessary to concentrate dust into layers, and may record a different time period; surface age estimates for the SPLD are on the scale of several to tens of Myr [*11*].

The high reflectance of Planum Australe [*4*], coupled with the observed H/L near unity (implying minimal interference at these radar frequencies) and lack of near-surface reflectors, suggests that this portion of the SPLD most closely resembles reflections off a smooth, planar water ice target, and may be the best location for radar calibration (in agreement with [*12*]).

The localized SPLD regions characterized by brighter subsurface echoes than the surface reflection are of interest. Presumably the CO_2 deposits present in these regions are capped by a sublimation lag; if these lag deposits are rougher than other ice-dominated regions of the SPLD, their enhanced scattering properties could lower the surface echo. A rugged surface overlying a reflector experiencing coherent interference could explain why a radargram has a brighter subsurface reflection than the surface echo. Constraining how subsurface reflectors can have greater returned power than the surface reflection has implications for the recent identification of subglacial lakes in MARSIS data [*13*, *14*]. Additionally, better understanding non-idealized radar scattering properties of ice-rich targets provides important context to prepare for the RIME and REASON analyses of the icy Galilean satellites.

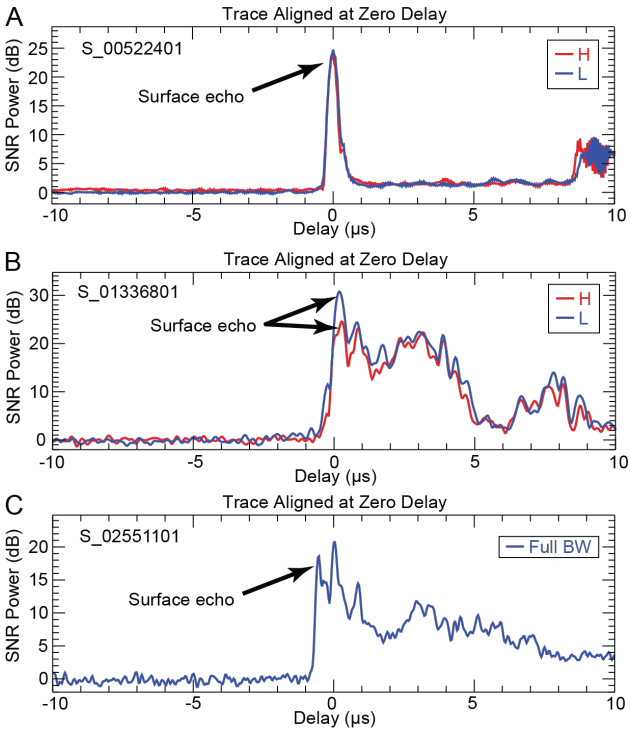

Figure 2. (A) H/L ~0 dB in Planum Australe. (B) H/L can reach ±6 dB in Gemina Lingula due to interference between closely spaced near-surface layers. (C) SPLD non-unity H/L values correlate with locations where subsurface reflections exceed the surface reflection (full bandwidth data). Extent of tracks shown in **Figure 1**.

Acknowledgments: This work is supported by MDAP grant #80NSSC20K1051.

References: [1] Plaut et al., (2007) *Science*. **316**, 92–95. [2] Phillips et al., (2009) *Science*. **320**, 1182–1185. [3] Putzig et al., (2009) *Icarus*. **204**, 443–457. [4] Campbell et al., (2021) *Icarus*. **360**, 114358. [5] Jawin et al., (2022) *GRL*. **49**, 17, e2022GL099896. [6] Seu et al., (2007) *JGR*. **112**. [7] Campbell et al., (2018) *GRL*. **45**, 1759–1766. [8] Phillips et al., (2011) *Science*. **332**, 838–841. [9] Bierson et al., (2016) *GRL*. **43**, 4172–4179. [10] Landis et al., (2016) *GRL*. **43**, 3060–3068. [11] Herkenhoff et al., (2000) *Icarus*. **144**, 243–253. [12] Grima et al., (2012) *Icarus*. **220**, 84–99. [13] Orosei et al., (2018) *Science*. **361**, 490–493. [14] Lalich et al., (2022) *Nat. Astron.* **6**, 1142–1146.